DEVELOPMENTAL DYNAMICS 211:109–121 (1998)

Targeted Disruption of the Mouse Villin Gene Does Not Impair the Morphogenesis of Microvilli

KATHLEEN I. PINSON,[1] LAURA DUNBAR,[1] LINDA SAMUELSON,[2] AND DEBORAH L. GUMUCIO[1]*
[1]*Department of Anatomy and Cell Biology, University of Michigan, Ann Arbor, Michigan*
[2]*Department of Physiology, University of Michigan, Ann Arbor, Michigan*

ABSTRACT **The small intestine is functionally dependent on the presence of the brush border, a tightly packed array of microvilli that forms the amplified apical surface of absorptive cells. In the core of each microvillus, actin filaments are bundled by two proteins, villin and fimbrin. Previous in vitro studies using antisense approaches indicated that villin plays an important role in the morphogenesis of microvilli. To examine the in vivo consequences of villin deficiency, we disrupted the mouse villin gene by targeted recombination in mouse embryonic stem cells. A β-galactosidase cDNA was also introduced into the villin locus by the targeting event. Homozygous villin-deficient mice are viable, fertile, and display no gross abnormalities. Intact microvilli are present in the small intestine, colon, kidney proximal tubules, and liver bile canaliculi. Although subtle ultrastructural abnormalities can be detected in the actin cores of small intestinal microvilli, localization of sucrase isomaltase, brush border myosin I, and zonula occludens I to the microvillar surface of the small intestine is normal. Thus, in vivo, villin plays a minor or redundant role in the generation of microvilli in multiple absorptive tissues. *Dev. Dyn. 1998;211:109–121.***

Key words: homologous recombination; embryonic stem cells; small intestine; brush border development; β-galactosidase

INTRODUCTION

Absorptive epithelial cells exhibit a structural polarity that facilitates their function. In the intestine, the apical surfaces of such cells are studded with approximately 1,000 microvilli, greatly amplifying the surface area available for absorption and providing a specialized domain for membrane-bound proteins (proteases, disaccharidases, transporters), which carry out the absorptive process. Together with the underlying terminal web, this dense lawn of uniform microvilli forms a distinct apical structure called the brush border. Other epithelia, including embryonic visceral endoderm as well as adult large intestine, kidney proximal tubules, hepatocytes, and portions of the reproductive tract, also exhibit microvilli, although these are structurally more variable than those of the intestine. The ultrastructure and biochemical composition of microvilli, especially those of the intestinal brush border, have been extensively investigated (for review, see Heintzelman and Mooseker, 1992). However, the molecular mechanisms that underlie the formation of microvilli and the precise functional roles of the proteins that comprise these structures are still not completely understood.

Intact intestinal brush borders can be readily isolated (Bretscher and Weber, 1978; Bretscher, 1981b). Predominant components of the isolated microvillar cores include actin and three actin-binding proteins: villin (95 kD), fimbrin (68 kD), and a 110-kD complex composed of calmodulin and brush border myosin I (BBMI). Whereas BBMI appears to comprise, at least in part, the lateral arms that bridge the bundled actin core to the plasma membrane (Coluccio and Bretscher, 1989), villin and fimbrin bundle actin filaments within the microvillar core itself. Fimbrin (also called plastin) is a member of a gene family that includes three closely related proteins: L-fimbrin, T-fimbrin, and I-fimbrin (Lin et al., 1993, 1994). Of these, I-fimbrin appears to be brush border-specific. Villin is encoded by a single copy gene in human (Pringault et al., 1991) and in mouse (Rousseau-Merck et al., 1988), and is a calcium-regulated member of the gelsolin family. This family of proteins, which also includes fragmin and severin, shares a homologous structural domain that acts to sever actin (Arpin et al., 1988). Like gelsolin, villin can nucleate, sever and cap actin (Craig and Powell, 1980; Glenney et al., 1981b; Janmey and Matusudaira, 1988). However, villin is unique among family members in its ability to bundle F-actin. An actin-binding site in the villin "headpiece," a unique C-terminal domain, acts in conjunction with a second actin-binding site in the "core" domain to confer bundling activity to the villin protein (Glenney and Weber, 1981; Glenney et al., 1981b). In vitro, villin bundles actin filaments at low calcium concentrations ($<10^{-7}$ M), whereas it severs, nucleates, and caps actin at high ($>10^{-6}$ M) levels of calcium (for review, see Mooseker, 1985). These regulatory features suggest that villin is more than a simple

Grant sponsor: National Institutes of Health; Grant number: R29 HD28620.
*Correspondence to: Deborah L. Gumucio, University of Michigan, Department of Anatomy and Cell Biology, 5793 Medical Science II, Ann Arbor, MI 48109-0616. E-mail: dgumucio@umich.edu
Received 15 September 1997; Accepted 8 October 1997

structural protein and may play a dynamic role in microvillar formation and/or maturation.

In vitro, villin and fimbrin each can form actin bundles independently (Bretscher and Weber, 1980; Bretscher, 1981a; Glenney et al., 1981a; Matsudaira et al., 1983). Thus, it is not clear whether these two proteins serve separate or overlapping roles in brush border formation. Transfection experiments in cultured CV-1 fibroblasts have supported the idea that villin plays a key role in this process. Normally, CV-1 cells lack villin and possess short, sparse, unorganized microvilli. However, in CV-1 cells transfected with a villin cDNA, stress fibers are disrupted, and numerous apical processes resembling the long microvilli of the intestine are formed (Friederich et al., 1989). The ability of I-fimbrin to modify the cytoskeleton of transfected CV-1 cells has not been tested, but overexpression of T- or L-fimbrin in these cells does not result in the formation of microvilli (Arpin et al., 1994).

More recently, it has been shown that villin is required for the establishment of brush border microvilli in CaCo2 cells. Expression of villin antisense mRNA in this colonic cell line blocks the formation of microvilli usually seen when these cells are induced to differentiate in culture (Costa de Beauregard et al., 1995). In addition, the intestinal enzyme sucrase isomaltase fails to localize to the apical plasma membrane in these brush border-impaired cells.

The fact that microvillar formation may be induced or inhibited by altering villin expression levels suggests that this protein plays a major role in establishing and/or maintaining microvillar structures. To examine directly whether villin is required for the morphogenesis of microvilli in the intestine or in other absorptive epithelia, we have disrupted the mouse villin gene by homologous recombination in embryonic stem (ES) cells. Surprisingly, analysis of mutant mice revealed intact microvilli in all absorptive tissues examined, indicating that villin is not required for microvillar morphogenesis or maintenance in vivo.

RESULTS

Targeted Disruption of the Mouse Villin Gene

The targeting vector was designed such that homologous recombination results in the replacement of 4.6 kb of villin genomic sequence (containing part of exon 1, all of exons 2 and 3, and the intervening introns) with the β-galactosidase and the neomycin-resistance cassettes (Fig. 1a). Following electroporation and G418 selection, 280 colonies were screened on Southern blots. Successful targeted recombination was demonstrated for eight clones (Fig. 1b). Four clones were injected into mouse blastocysts, and two (B3 and E2) produced germline chimeras. Offspring of chimeras generated from both targeted clones were examined as described below for possible effects of villin loss.

Loss of Villin Protein and mRNA

Total protein was isolated from intestinal epithelia of wild type mice and mice heterozygous and homozygous for the targeted allele and was analyzed by Western blotting. To confirm the loss of the villin protein, blots were probed with a monoclonal antibody that recognizes the C-terminal headpiece (Dudouet et al., 1987), the domain responsible for the actin-bundling activity of villin. The villin protein (95 kD) was clearly detectable in wild type mice (Fig. 2a, lane 1) and in heterozygotes (Fig. 2a, lane 2) but not in mice homozygous for the targeted allele (Fig. 2a, lane 3). In addition, no novel protein species were detected in mice heterozygous or homozygous for the targeted allele.

Villin mRNA levels were examined by Northern analysis of total RNA from small intestine and kidney of wild type, heterozygote, and homozygous mutant adults. Blots were hybridized with a villin cDNA probe spanning exons 7–18. In intestinal RNA of wild type mice, two villin transcripts (3.8 kb and 3.4 kb) were detected (Fig. 2b, lane 1). These transcripts result from the use of two alternative polyadenylation signals located 400 bp apart (Ezzell et al., 1992). The major transcript (3.8 kb) was reduced in heterozygotes (Fig. 2b, lane 2) and was absent in homozygotes (Fig. 2b, lane 3). In homozygotes, a low-abundance transcript was detected that appeared to comigrate with the 3.4-kb mRNA. However, Northern analysis using multiple villin probes revealed that this transcript contains sequences 3′ to the first villin polyadenylation signal (not shown); therefore, it does not represent the wild type 3.4-kb transcript. Further analysis by reverse transcription polymerase chain reaction (RT-PCR; Fig. 2c) indicated that this transcript is generated from alternative splicing of the 5′ donor region of the villin nontranslated exon (NTE) to the acceptor region of exon 4, eliminating the normal villin translational start codon. The resulting mRNA is 338 bp shorter than the 3.8-kb transcript, accounting for its apparent comigration with the 3.4-kb villin transcript. This alternative transcript contains 11 in-frame ATG codons that possess surrounding sequence context conforming to a Kozak consensus or weak variant thereof (Kozak, 1996). However, no corresponding truncated protein products were detected in extensive Western analyses. Therefore, hereafter, we refer to the homologously targeted mice as villin-deficient mice.

Villin-Deficient Mice Are Viable and Fertile

A total of 40 heterozygous offspring were obtained from three chimeric males produced by injection of the B3 cell line and four males produced from injection of the E2 cell line. A balanced sex ratio was observed among heterozygotes. No gross defects were seen in the heterozygous mice during postnatal growth, weaning, and maturation.

Offspring from heterozygote crosses were viable, and null mice were obtained with expected Mendelian frequency (19 wild type, 42 heterozygous, 22 nulls). Among

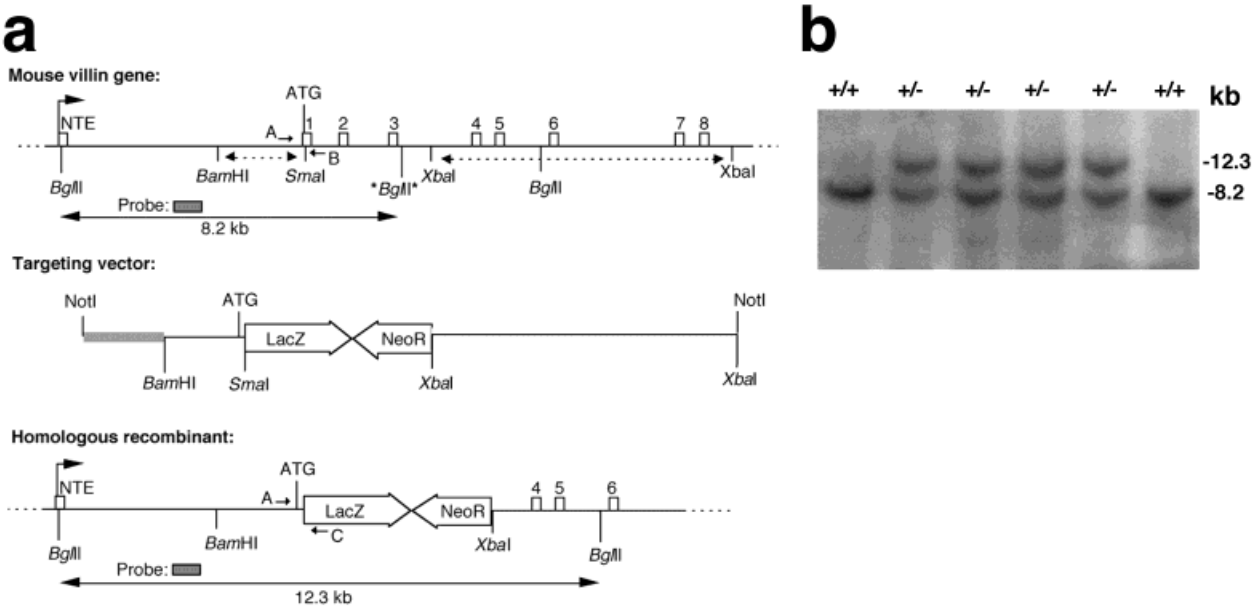

Fig. 1. Targeting of the mouse villin locus in embryonic stem (ES) cells. **a:** Mouse villin gene structure. The 5′ region of the mouse villin gene contains an additional nontranslated exon the (NTE), 5′ to the reported human exon 1 (L. Dunbar, in preparation). A partial restriction map of the region spanning the NTE and exons 1 through 8 is shown, and the location of polymerase chain reaction (PCR) primers used to amplify the endogenous villin locus (AB) is indicated. Targeting vector: Fragments of 2.1 kb (5′) and 7.2 kb (3′) from the villin genomic region (dotted lines) flank a β-galactosidase cDNA and neomycin resistance cassette (see Experimental Procedures). Vector sequence is designated by a shaded line 5′ to the *Bam*HI site. Homologous recombinant: Targeted deletion of the **Bgl*II* site just 3′ to exon 3 results in a 12.3-kb *Bgl*II fragment, which can be distinguished from the 8.2-kb endogenous *Bgl*II fragment by using a 500-bp *Hind*III/*Hind*III probe (shaded rectangle). The location of PCR primer set AC, which amplifies the targeted allele, is indicated. **b:** Southern analysis of DNA from targeted and wild type ES cells: Genomic DNA was digested with *Bgl*II, and blots were hybridized with the probe indicated in a. Wild type ES cells (first and last lanes) are represented by a single band at 8.2 kb. In cells heterozygous for the correct targeted recombination, a second band at 12.3 kb is observed. Proper recombination at the 3′ end of the targeted allele was also verified by Southern analysis (data not shown).

the nulls, sex ratios were balanced. Wild type, heterozygous, and homozygous litter mates were weighed at weaning (3 weeks of age), and increases in weight were recorded over a period of approximately 3 weeks. No significant differences were detected in weight or in the rate of weight gain (data not shown). Both male and female homozygously targeted mice were fertile.

Effect of Villin Deficiency on Microvillar Structure

The ultrastructure of microvilli in the small intestine of mutant mice was examined by transmission electron microscopy (TEM). The central actin bundle forming the core of each microvillus, which was clearly detectable in wild type mice (Fig. 3a,b) was diffuse in mutant animals (Fig. 3c,d). In addition, the terminal web located at the base of the microvilli often appeared to be thicker and less well organized in mutant mice. The thickening of the terminal web appeared to reflect a continuation of the actin core disruption as it extended toward the terminal web (the rootlet) rather than a disruption of the terminal web itself. These differences in core and terminal web structures were observed consistently in intestines processed from three null animals. It should be noted, however, that osmium tetroxide (the agent used in postfixation) has the potential to sever actin filaments (Maupin-Szamier and Pollard, 1978; Small and Langanger, 1981). This osmium-induced fracturing is inhibited by actin-binding proteins. Thus, it is not clear whether the loss of dense core bundles seen in mutant mice is a structural effect that results directly from villin loss or a secondary effect resulting from increased susceptibility to the severing activity of osmium.

TEM analysis was also performed to examine the ultrastructure of microvilli in other tissues of villin-deficient mice, including large intestine, kidney proximal tubules, and liver bile canaliculi. Intact microvilli were observed in all tissues examined (Fig. 4a–c).

Because villin is able to both sever actin and promote the growth of actin filaments in vitro (Bretscher and Weber, 1980; Craig and Powell, 1980), we tested whether the loss of villin would perturb microvillar length. Lengths of microvilli from wild type and villin-deficient mice were measured on photomicrographs of small intestine and colon epithelia, as described in Experimental Procedures. The results of this analysis are presented in Table 1. The range and standard deviation of microvillar measurements indicate that considerable variation in length was seen in the small intestine, even within a single wild type or mutant animal. Although the small number of animals analyzed precludes the application of statistical tests, the measurements suggest a possible trend toward shorter microvilli in the

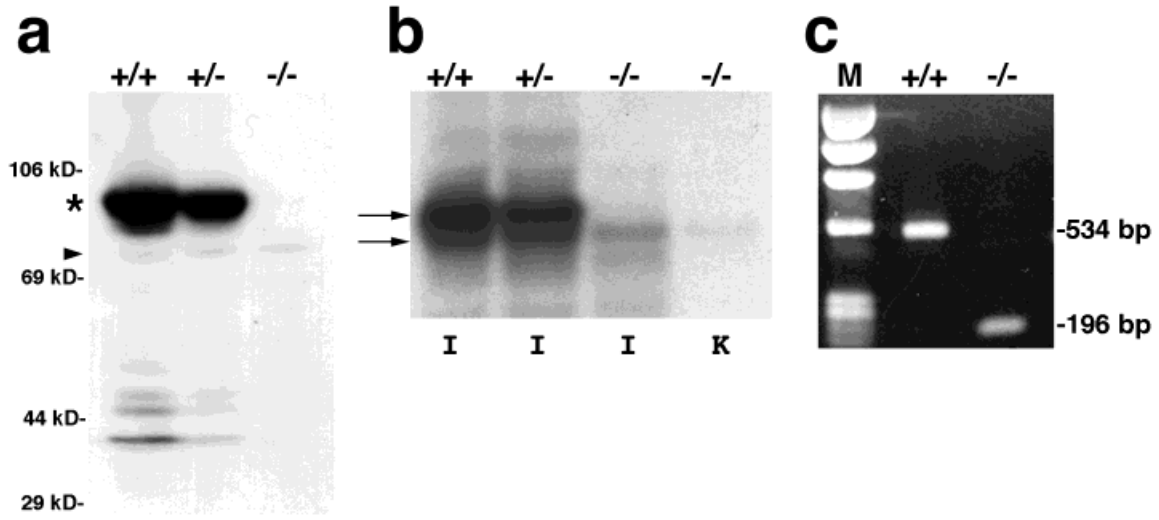

Fig. 2. Loss of villin protein and mRNA in mutant mice. **a:** Immunoblot of total protein (80 μg/lane) from the small intestine of wild type (+/+), heterozygous (+/−), and homozygous mutant (−/−) mice. Hybridization with the villin monoclonal antibody (BDID2C3) reveals the 95-kD villin protein (*). A smaller, nonspecific band (arrowhead) present in all three lanes demonstrates equal loading of protein samples. **b:** Northern blot analysis of villin mRNA from intestine (I) and kidney (K). Hybridization with a probe spanning villin exons 7–18 reveals two mRNA species (3.8 and 3.4 kb) in +/+ and +/− mice (arrows). In −/− mice, this probe detects a low-level transcript (16% compared with the total villin transcript signal present in the +/+ intestine, as determined by PhosphorImager analysis) at 3.35 kb in both intestine and kidney. **c:** PCR analysis of reverse-transcribed RNA from +/+ and −/− mice. By using primers in the villin NTE and exon 5, the expected 534-bp fragment was amplified from +/+ mice. This fragment was missing in RNA from −/− mice; instead, a smaller fragment (196 bp) was amplified by the same primers. Sequence analysis of the 196-bp product confirmed splicing between the donor site of the NTE and the acceptor site of exon 4. Marker (M): ϕX174 DNA digested with *Hae*III.

colon of villin-deficient mice. However, it is clear that loss of villin protein does not have a major effect on microvillar length.

Scanning electron microscopy (SEM) was carried out to determine whether loss of villin would delay formation or alter density of the microvillar brush border during embryonic development. Wild type and villin-deficient fetuses were examined each day during the time of active intestinal microvillar formation (13.5–17.5 days postcoitum; dpc). At 13.5 dpc, short, sparse microvilli were present on most cells, often projecting at odd angles from the cell surface (not shown). Through 15.5 dpc, considerable variability in microvillar density was noted both between animals and even within a small sample area from an individual animal (Fig. 5a,b). Chambers and Grey (1979) noted a similar lack of synchrony in the development of microvilli during chick embryogenesis. However, over time, the number and length of microvilli increased, and the overall appearance of the epithelial surface became more homogenous. By 17.5 dpc (Fig. 5c,d), the microvilli of the brush border in both wild type and mutant animals had achieved a level of confluence indistinguishable from the adult samples. No differences in the density of duodenal microvilli could be detected between wild type and villin-deficient mice at any fetal or adult time point sampled (Fig. 5; data not shown). Thus, the SEM analysis revealed no consistent alteration in the density or distribution of nascent microvilli nor in the timing of microvillar formation in villin-deficient animals.

Localization of Apical Markers in Villin-Deficient Mice

Earlier studies in CaCo2 cells had indicated that loss of villin mRNA leads to impaired apical localization of sucrase isomaltase (Costa de Beauregard et al., 1995). Therefore, we analyzed sucrase isomaltase localization in villin-deficient mice. An apical staining pattern indistinguishable from the wild type pattern was seen on immunostained sections by using an antisucrase isomaltase antibody (Fig. 6a,b). Thus, in vivo, villin is not required for proper apical localization of this enzyme.

Because subtle alterations in the core and terminal web region of the villin-deficient mice had been noted by using TEM, the distribution of other brush border proteins was also examined, including ZO-1, a protein found at the occludens junctions and brush border myosin I that links actin cores to the overlying plasma membrane of the microvilli. The immunostaining patterns of these two proteins were identical in wild type mice (Fig. 6c,e) and in villin-deficient mice (Fig. 6d,f), indicating that the loss of villin does not result in major changes in the cytoskeletal organization of the apical surface.

Expression of β-Galactosidase

The targeting vector was designed to place a β-galactosidase cDNA under the control of the endogenous villin promoter. Staining for β-galactosidase activ-

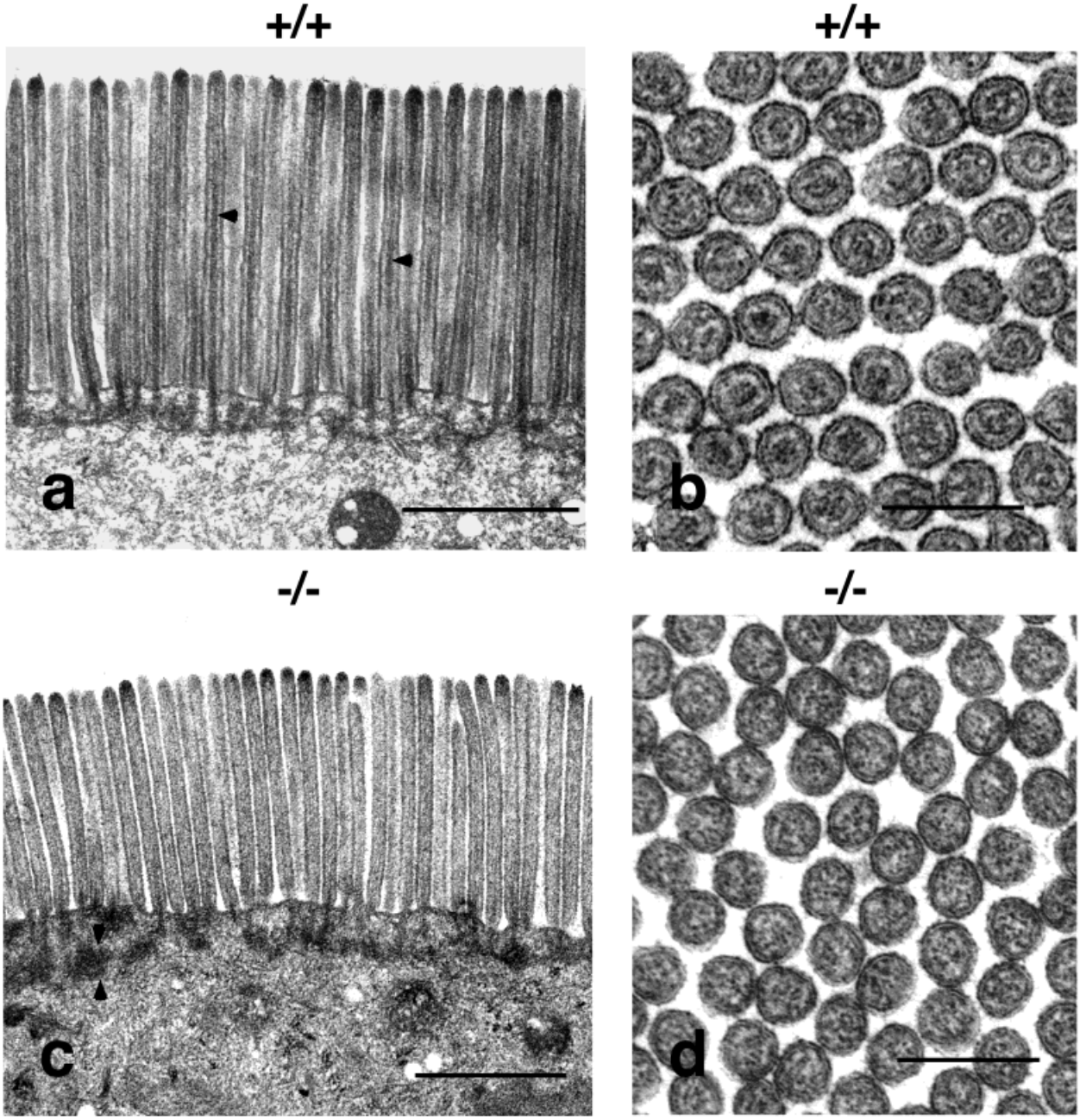

Fig. 3. Structural abnormalities in the actin core of microvilli from small intestines of villin-deficient mice. **a:** Microvilli in the small intestine of wild type mice (+/+) contain a dense actin core (arrowheads) visible by transmission electron microscopy. Cross-sectional profiles of wild type microvilli (**b**) reveal a tightly packed array of actin filaments. In villin-deficient mice (−/−), microvilli lack well-bundled actin cores (**c,d**) but appear structurally normal otherwise. Examination of the terminal web region (in the apical cytoplasm underlying the microvilli) reveals a change from a dense, localized filament staining (a) to a thicker, diffuse appearance (arrowheads in c). Junctional complexes appeared structurally normal in mutant mice (not shown). Scale bars = 1 μm in a,c, 200 nm in b,d.

ity in a villin-deficient 13.5-dpc embryo revealed expression of this marker in a tissue-specific pattern in the herniated intestine and in the embryonic yolk sac (Fig. 7a). Expression was sharply confined to the visceral endoderm of the latter (not shown). Staining was also detected in regions of the developing urogenital system. In a 13.5-dpc, heterozygous embryo (Fig. 7b), staining was detected in the kidneys, and a striking anterior border of staining was observed at the pyloroduodenal junction. Sections of small intestine from an adult chimeric animal revealed that β-galactosidase activity was restricted to epithelial cells lining the villi (Fig. 7c). In the chimera, cells in individual crypts were either entirely positive or entirely negative for β-

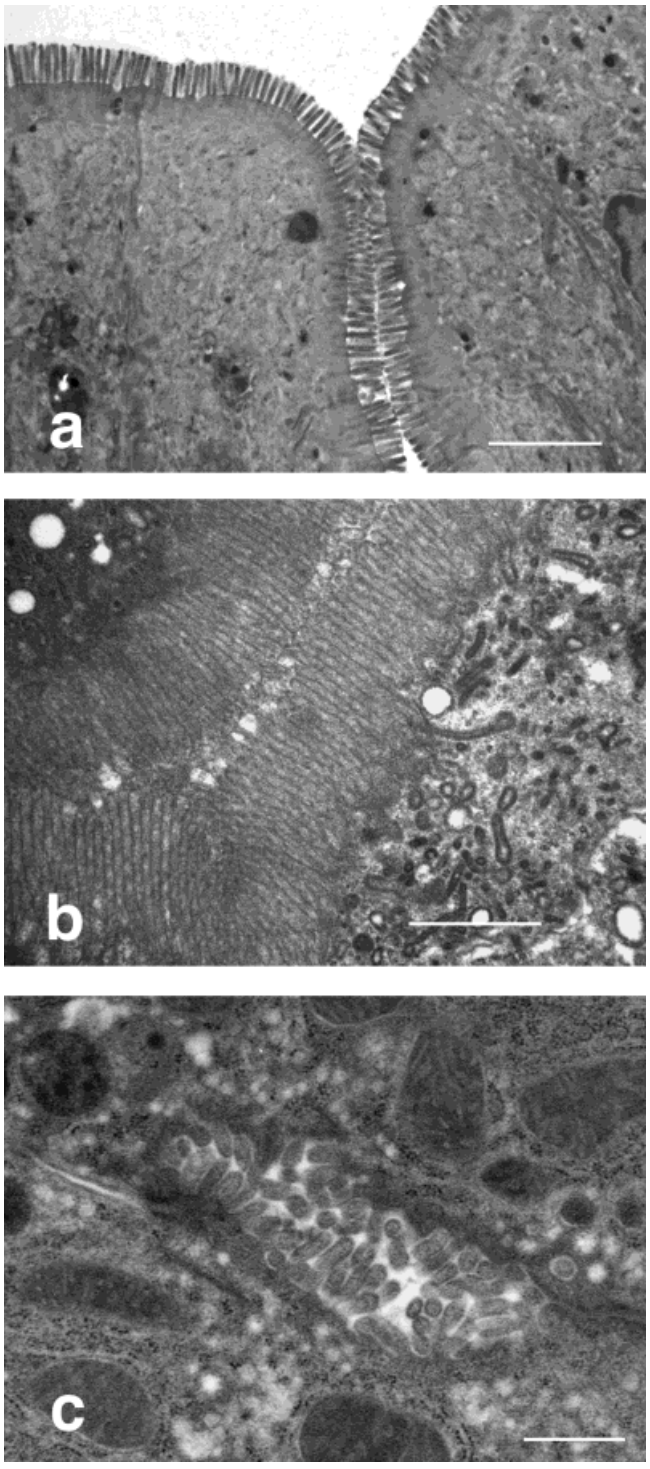

Fig. 4. Transmission electron microscopy demonstrates morphologically intact microvilli in several tissues. Microvilli are present on cells of the colon (**a**), on kidney proximal tubule cells (**b**), and on the bile cannalicular surface of hepatocytes (**c**) in villin-deficient animals. In each tissue, the microvillar structures seen in mutant mice were indistinguishable from those seen in wild type controls (not shown). Scale bars = 2 μm in a, 1 μm in b, 500 nm in c.

TABLE 1. Microvillar Lengths in Wild Type and Villin-Deficient Animals[a]

	Wild type (μm)	Villin-deficient (μm)
Small intestine		
x ± S.D.	1.0 ± 0.2	1.2 ± 0.3
Range	0.6 − 1.4	0.4 − 1.8
n	85	105
Colon		
x ± S.D.	0.61 ± 0.13	0.45 ± 0.10
Range	0.33 − 0.87	0.33 − 0.80
n	109	114

[a]±S.D., mean ± standard deviation; n, number of microvilli measured.

galactosidase activity. Positive crypts gave rise to blue staining cells that populated the surface of adjacent villi (Fig. 7c). This pattern is consistent with the known monoclonality of crypts (Schmidt et al., 1988). Comparison of this preliminary analysis of β-galactosidase expression in targeted mice with the known expression pattern of villin (Ezzell et al., 1989; Maunory et al., 1988, 1992) suggests that the genomic region between exon 1 and exon 4, which was deleted by the targeting event, does not harbor key regulatory elements.

DISCUSSION

This analysis of a targeted disruption of the mouse villin gene indicates that microvilli are formed in multiple absorptive tissues in the absence of villin. The highly ordered microvillar structure known as the brush border of the intestine, the considerably less well-organized microvilli that line hepatic bile canaliculi, as well as the long thin microvilli of kidney proximal tubule cells are all preserved in villin-deficient mice. Despite the fact that villin is among the first of the brush border proteins to be apically localized in the developing intestine (Ezzell et al., 1989), its loss produces no alterations in the timing or structural outcome of microvillar morphogenesis. These results indicate either that villin is dispensable or that another protein (or proteins) can effectively compensate for the loss of villin.

Although microvillar morphogenesis can proceed normally in the absence of villin, the possibility still exists that, under certain stressful processes, such as the remodeling of the intestinal surface following wounding (for review, see Health, 1996), villin could play a more prominent role. Interestingly, disruption of the gene for gelsolin (Witke et al., 1995), a protein that shares structural and functional homology with villin, causes impaired cellular migration and retards wound healing (O'Kane et al., 1996). The possibility that villin is required for the wound-induced remodeling of the intestinal epithelium either for breakdown of microvilli at the wound border or for the reestablishment of the brush border upon wound closure can now be directly tested in villin-deficient mice.

Based on previous biochemical analyses of the villin protein, it was predicted that villin is involved in the

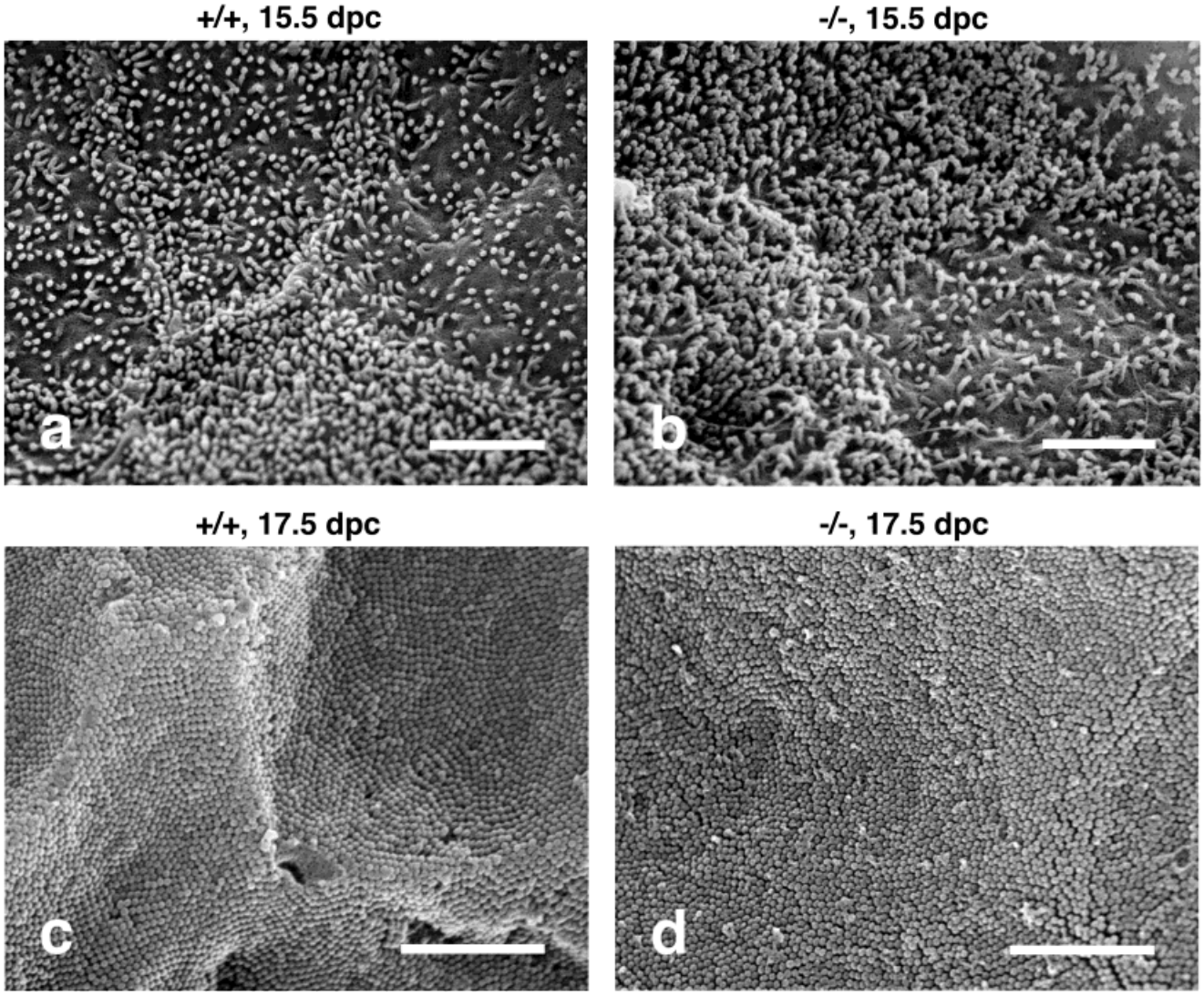

Fig. 5. **a–d:** Formation of intestinal microvilli in wild type and villin-deficient mice, as revealed by scanning electron microscopy (SEM). At 15.5 days postcoitum (dpc), regional differences are observed in microvillar density, but wild type (+/+; a,c) and mutant (−/−; b,d) samples are indistinguishable in terms of density and microvillar external structure. By 17.5 dpc (c,d), the intestinal surface is covered with microvilli in wild type and villin-deficient mice. Adult small intestinal surfaces are similar in appearance to those shown in c and d (not shown). Scale bars = 2 μm.

regulation of microvillar length. For example, in vitro studies demonstrated that villin promotes unidirectional assembly of F-actin filaments. If villin is important for the early nucleation of actin filaments during the process of microvillar formation, as proposed by Ezzell et al. (1989), then shorter microvilli might be predicted in villin-deficient mice. Alternatively, longer microvilli might be expected if the severing activity of villin is important in the control of microvillar length (Coluccio and Bretscher, 1989). However, measurements of microvillar lengths in colon and small intestine of wild type and villin-deficient mice revealed only a slight tendency for shorter microvilli in the colon. In the small intestine, the high degree of variability in lengths of small intestinal microvilli even in wild type mice makes this a difficult point to define clearly, but small intestinal microvilli from null mice appear no more variable and clearly are not demonstrably longer or shorter than wild type microvilli. Thus, neither the nucleating nor the severing activity of villin are essential for control of microvillar length in vivo.

At the ultrastructural level, the loss of villin results in reproducible differences in the organization of actin core bundles. Microvilli in wild type mice exhibit regular, tightly packed cores of bundled actin filaments. In mutant mice, no organized core structure is present, although actin filaments are clearly visible. A similar change in core structure was seen in CaCo2 cells

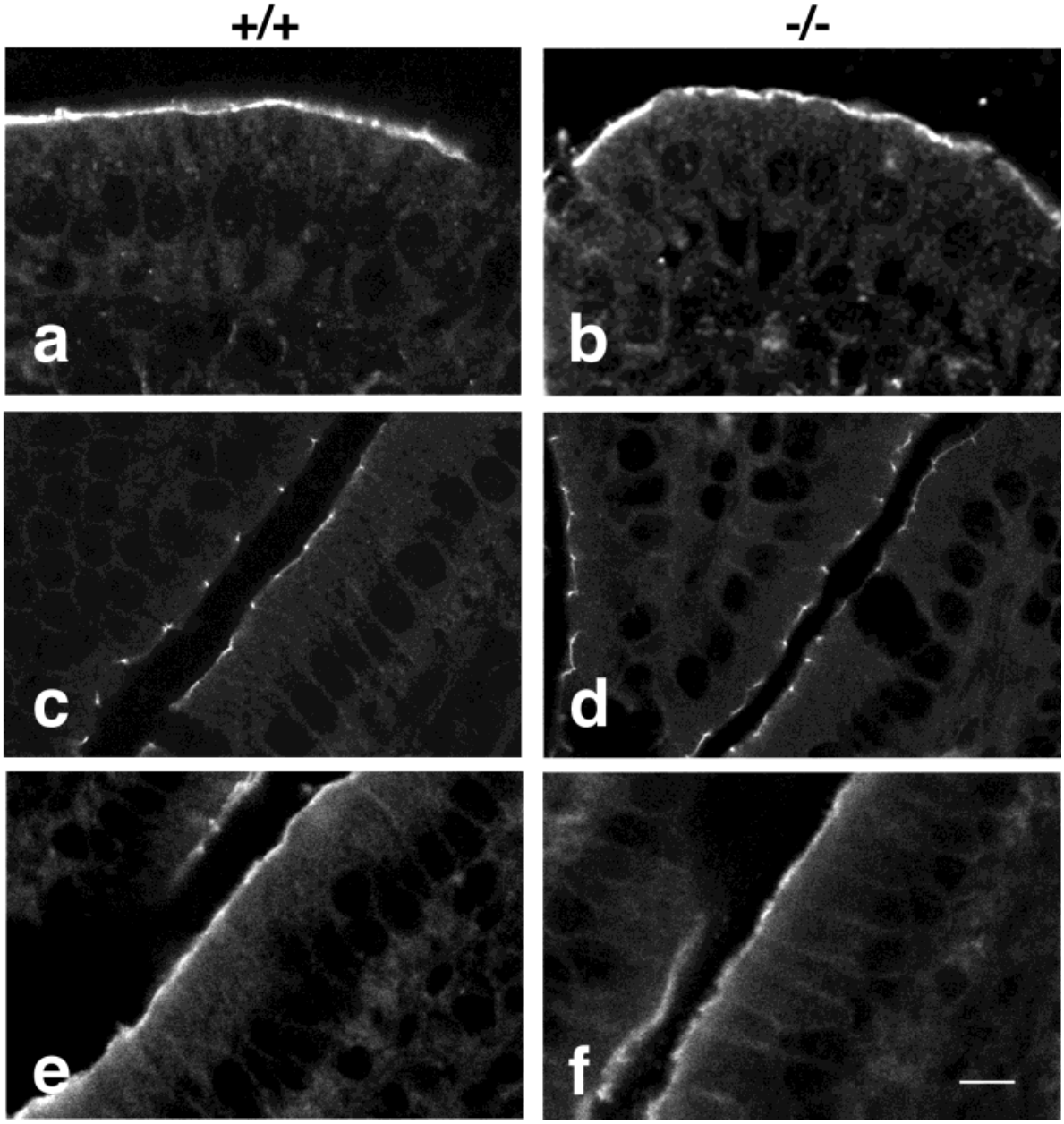

Fig. 6. **a–f:** Immunochemical localization of brush border enzymes and structural proteins appears normal in villin-deficient mice. Comparison of the small intestine of wild type (a,c,e) and villin-deficient (b,d,f) mice reveals no differences in the localization or apparent concentration of sucrase isomaltase (a,b), zonula occludens I (c,d), or brush border myosin I (e,f). Immunostaining was performed as described in Experimental Procedures, and images were obtained by using confocal microscopy. Scale bar = 10 μm.

exposed to antisense villin message. Rudimentary microvilli seen in these cells lacked discrete actin bundles (Costa de Beauregard et al., 1995). Although in vitro reconstitution assays suggest that cores with similar packing densities can be formed by villin plus actin and by fimbrin plus actin (Glenney et al., 1981a), these results in null mice indicate that the formation of a tightly packed core structure requires villin.

In contrast to the actin core disruption, several other effects of antisense-induced villin loss in CaCo2 cells were not recapitulated in vivo. Specifically, significant alterations in microvillar density and length were observed after villin ablation in CaCo2 cells but not in villin-deficient mice; and, although sucrase isomaltase protein was not targeted correctly to the apical membrane in antisense-expressing CaCo2 cells, the apical localization of this disaccharidase was indistinguishable in wild type and villin-deficient mice in vivo. Although the specific factors that underlie these differential responses to villin loss are unknown, several

COLOR

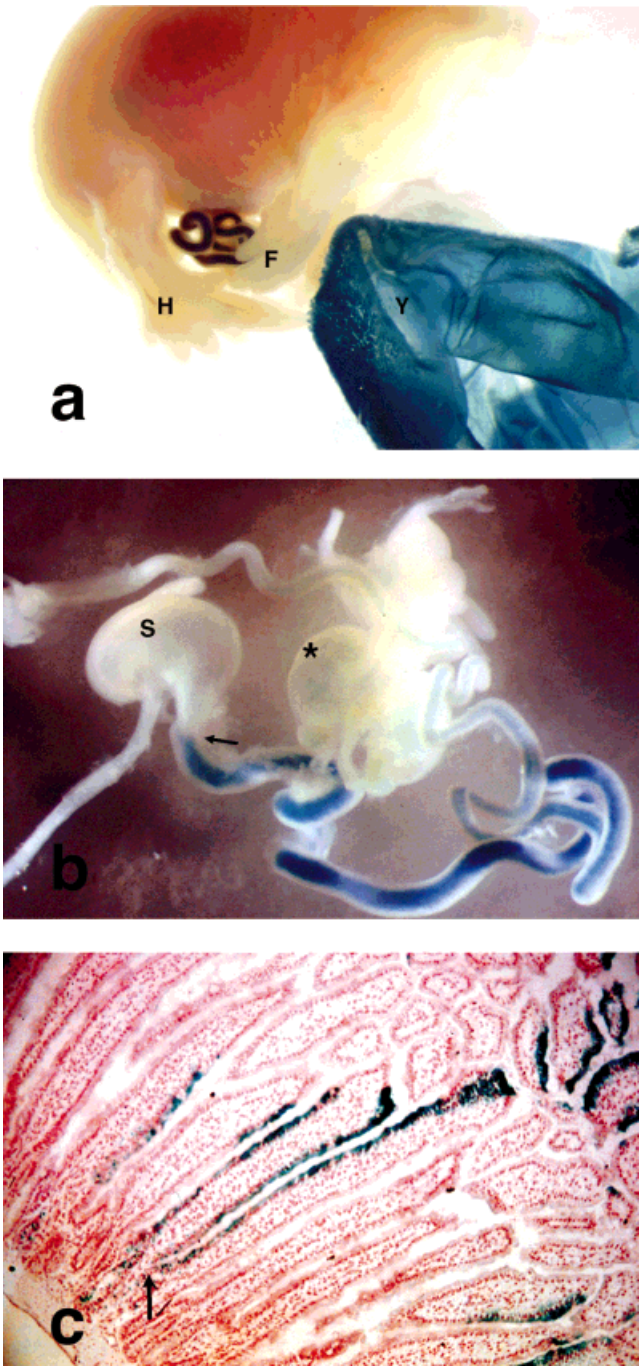

Fig. 7. β-Galactosidase expression in embryonic and adult tissues. **a:** A 13.5-dpc, homozygous null embryo shows intense staining of the herniated intestine and yolk sac (H, hindlimb; F, forelimb; Y, yolk sac). **b:** Viscera removed from a heterozygous 13.5-dpc embryo. A sharp boundary of β-galactosidase activity occurs at the pyloroduodenal junction (arrow), and faint staining can be detected in the kidney (*) (S, stomach). **c:** β-Galactosidase expression in the small intestine of an adult chimera. Arrow indicates the top of a +/− crypt (out of plane), which is populating the epithelial surface of two villi.

considerations seem particularly relevant. First, it is likely that the capacity of developing intestinal cells in vivo to respond to (or compensate for) villin loss is far greater than that of cultured cells in vitro (which are capable of a more restricted range of dynamic states). Second, CaCo2 cells are derived from a colonic adenocarcinoma and, as such, exhibit transformed properties that do not mirror the physiological (or three-dimensional) state of the small intestine in vivo.

Another important difference between CaCo2 cells and fetal or adult intestinal cells is the concentration of other actin-binding proteins that could potentially compensate for villin loss. For example, three fimbrin isoforms exist, I-, T-, and L-fimbrin. Although all three isoforms are expressed in developing gut, T- and L-fimbrin disappear before brush border maturation (17.5 dpc), leaving I-fimbrin as the only isoform associated with the microvillar surface in normal adult intestine (Chafel et al., 1995). In CaCo2 cells, however, the ratios of the fimbrin isoforms do not appear to directly reflect the ratios seen in vivo in either fetal or adult intestine. T- and L-fimbrin are expressed at extremely high levels in CaCo2 cells, whereas I-fimbrin in these cells is found at levels much lower than those seen in either the colon or the small intestine (Lin et al., 1994). It is possible that, due to the different fimbrin isoform ratios in CaCo2 cells, the sensitivity of microvillar structures to villin loss is enhanced in this environment.

The present data do not resolve definitively whether villin plays a very minor role in brush border formation or whether other molecules compensate for its absence. Because its expression correlates most closely with brush border formation, I-fimbrin has been postulated to be the most important fimbrin isoform in microvillar morphogenesis (Chafel et al., 1995). Thus, it is possible that I-fimbrin is the molecule that substitutes for the absent villin protein in this tissue. To rule out an increase in I-fimbrin mRNA as a potential mechanism for compensation, we measured the concentration of I-fimbrin mRNA in intestines of wild type and villin deficient mice. No increase in I-fimbrin mRNA was detected (data not shown), although a possible alteration in the pattern of cellular localization of I-fimbrin in mutant mice has not been excluded. Other actin binding proteins (e.g., ezrin; Berryman et al., 1995) present in lower concentrations in microvilli could also potentially contribute to the generation of microvilli in the absence of villin.

The results of this analysis of villin-deficient mice emphasize the complex and possibly redundant nature of the process of microvillar formation in absorptive tissues. When targeted disruptions of additional microvillar actin-binding proteins are accomplished and animals that lack multiple such proteins are produced, more information about the molecular order of the process of microvillar morphogenesis will accrue. The villin-deficient mouse described here will play an important role in the further analysis of this process.

EXPERIMENTAL PROCEDURES

Construction of the Targeting Vector

Two overlapping lambda clones containing the villin genomic region were isolated from a mouse strain

129/SVJ genomic library (Stratagene, La Jolla, CA), by hybridization with a probe derived from the human villin cDNA (exons 1–3). Exons were localized to specific restriction fragments on Southern blots and were partially sequenced. The targeting vector was assembled from the following components (5′ to 3′): a 2.1-kb *Bam*HI/*Sma*I fragment from the villin gene; the LacZ gene (encoding β-galactosidase) from the pCH110 vector (Genbank U13845); a neomycin resistance cassette driven by the PGK promoter (in reverse orientation with respect to the villin promoter); and a 7.2-kb *Xba*I fragment from the villin gene (Fig. 1a). The targeting vector was linearized with *Not*I prior to electroporation.

Transfection and Screening of ES cells

R1 ES cells (Nagy et al., 1993) were maintained on mitotically inactive mouse embryonic fibroblast feeder layers (Wurst and Joyner, 1993). Cells were maintained in Dulbecco's modified Eagle medium containing 15% fetal calf serum (JRH Biosciences, Lenexa, KS), 0.1 mM β-mercaptoethanol, 50 units/ml penicillin, 50 μg/ml streptomycin, and 1,000 units/ml leukemia inhibitory factor (GIBCO, Gaithersburg, MD).

ES cells (1×10^7) were electroporated with 20 mg of linearized plasmid DNA at 320 V and 250 μFarads by using a GenePulser (Bio-Rad Laboratories, Hercules, CA). Cells were plated at a density of 1×10^7 cells per 100-mm plate on mitotically inactivated G418-resistant mouse embryonic fibroblast feeder layers (Doetschman, 1994). At 24 hours, 200 μg/ml active G418 were added to the culture medium. Surviving clones were picked 7–10 days later onto 96-well plates containing feeder layers. Expansion, freezing, and thawing were as described (Kendall et al., 1995).

DNA was isolated from cells grown on 96-well plates (Ramirez-Solis et al., 1992), and correct targeting was assessed on Southern blots (Fig. 1b). Following digestion with *Bgl*II, genomic DNA was separated on a 0.7% agarose gel and transferred to nylon membrane (Hybond N; Amersham, Arlington Heights, IL). Probes were gel isolated and radiolabeled by random priming using the Megaprime DNA labeling system (Amersham).

Generation and Screening of Villin-Deficient Mice

Four independent correctly targeted ES clones were injected into C57BL/6J blastocysts, which were then transferred to pseudopregnant CD1 females by the University of Michigan Transgenic Animal Core to obtain chimeras (Bradley, 1987). All experiments were conducted in accord with the principles and procedures outlined in the National Institutes of Health "Guidelines for the Care and Use of Experimental Animals." Male offspring with >70% agouti coat color were bred to C57BL/6J female mice (Jackson Laboratories, Bar Harbor, ME). Genotypes of pups were determined by PCR using a 5′ primer, 5′-TGCACTGGCCTAAAGCTCAC-3′′ (primer A), which binds intronic sequence 5′ to villin exon 1 and two alternative 3′ primers; 5′-ACCTC-GATCCTCCATATCTG-3′ (primer B), which binds exon 1 sequence present only in the villin wild type allele; or 5′-CGACAGTATCGGCCTCAGG-3′ (primer C), which binds within the LacZ gene of the targeted allele (Fig. 1a). Primer set AB generated a 600-bp product (wild type allele), and primer set AC produced a 900 bp fragment (targeted allele).

Western Analysis

Total protein was isolated from mouse small intestinal epithelial cells, as described previously (Craig and Lancashire, 1980; Gustin and Goodman, 1981; as modified by Dudouet et al., 1987). The lysis buffer was further modified to contain 20 mM Tris, pH 8.8; 7.5 mM $CaCl_2$; 1 mM phenylmethylsulfonyl flouride; 1 μg/ml antipain; 1 μg/ml pepstatin; and 15.7 μg/ml benzamidine. Protein concentration was determined by using the Lowry protein assay (Bio-Rad). Following electrophoresis and blotting, proteins were detected by using a monoclonal antibody against villin, BDID2C3 (Immunotech, Inc., Westbrook, ME) in combination with enhanced chemiluminescence (ECL; Amersham). This antibody is specific for the villin headpiece, the most C-terminal structure (Dudouet et al., 1987).

RNA Analysis

To isolate total RNA from the small intestine of adult mice, approximately 10 cm of tissue distal to the pyloroduodenal junction were excised, flushed with phosphate-buffered saline (PBS), and homogenized in 10 volumes TRIzol Reagent (GIBCO). Portions of adult kidney were also removed and homogenized as described above. Following phase separation and precipitation, redissolved RNA (10 μg/sample) was electrophoresed on a 1.3% agarose/1X MOPS gel containing 0.5% formaldehyde and transferred to nylon membrane (Hybond N; Amersham). Northern blots were hybridized with the following probes: 1) hypoxanthine phosphoribosyltransferase (HPRT) cDNA PCR product (Keller et al., 1993) as a control for RNA loading, 2) villin exons 7–18 (1.5-kb PCR fragment from cDNA), 3) villin 3′ untranslated region [UTR; a 313-bp *Nco*I/*Dra*I fragment from American Type Culture Collection (ATCC) no. 830331/Genbank W57229] described previously as the "G′ fragment" (Ezzell et al., 1992), 4) I-fimbrin (500-bp *Eco*RI fragment from ATCC 105654/Genbank T29230). Probes were gel isolated and radiolabeled as described above.

For reverse transcription-PCR (RT-PCR) analysis of villin transcripts, total intestinal RNA from wild type or homozygous targeted mice was isolated as described and reverse transcribed by using an oligo-dT primer. PCR amplification was carried out by using a forward primer in the nontranslated exon (NTE; 5′CTC GGA TCC CTT CCT AAG ATC TCC C) and a reverse primer in exon 5 (5′ AAC TCT TCC AGG ACA TTT CC). PCR products were cloned and sequenced.

TEM and SEM analysis

Adult mice were fasted overnight prior to TEM analysis. Small intestinal (3 cm distal to pyloroduodenal junction), colon (1 cm distal to caecum), kidney, or liver samples were excised and cut into 1-mm pieces in Karnofsky's fixative (2% paraformaldehyde, 3% glutaraldehyde) in 0.1 M cacodylate buffer (0.12 M sucrose/2 mM $CaCl_2$, pH 7.3). Tissues were fixed for 4 hours at room temperature, rinsed overnight in cacodylate buffer (4°C), and postfixed in 1% osmium tetroxide/0.1 M cacodylate buffer (2 hours at room temperature). Following washing and dehydration, tissues were embedded in Epon araldite (Polysciences, Inc., Warrington, PA). Seventy-nanometer sections obtained on a Reichart Ultracut microtome were poststained (uranyl acetate and lead citrate) and viewed on a Philips CM-100 transmission electron microscope (Philips Electronics Instruments, Inc., Eindhoven, The Netherlands).

To determine whether the loss of villin affects microvillar length in the small intestine, electron photomicrographs were taken of cells on the upper one-third of the villus (avoiding the microvillar tip). Two wild type and two villin-deficient mice were sampled, and three to five villi were examined per animal. Only cells in which the plane of section included the entire microvillar length were photographed. From each photomicrograph, the lengths of five microvilli were measured.

A similar analysis was conducted of microvillar length in the colon using tissue from two wild type and two villin-deficient mice. In this case, measurements were taken along the entire apical surface (excluding only the crypts). Five microvilli were measured in each region photographed (approximately ten regions/mouse).

For SEM, timed-pregnant females from heterozygous matings were sacrificed by cervical dislocation. The day of vaginal plug was taken as 0.5 days dpc. Embryos were removed from the uterus and fetal membranes, crown-rump length was measured, and heads were removed for DNA isolation and genotyping by PCR. Tissues (proximal duodenum or proximal colon) were removed and fixed in Karnofsky's fixative, as described above. Following washes in 0.1 M cacodylate buffer, tissues were further dissected into 0.5-1 mm pieces and dehydrated in ethanol followed by hexamethyldisilazane. Dried samples were then fractured, mounted, coated with gold/palladium under vacuum, and viewed on a scanning electron microscope (DS-130; International Scientific Instruments, Inc., Santa Clara, CA). Adult mice were also killed for SEM analysis of the proximal duodenum and colon. Tissue was processed as described above.

Immunocytochemistry

Primary antibodies used for immunostaining included mouse anti-chicken brush border myosin I (1:500; Chemicon International, Temecula, CA), rat anti-mouse zonula occludens I (ZO-1; 1:500; Chemicon), and rabbit anti-rat sucrase isomaltase (1:250; gift from Dr. K. Yeh, Louisiana State University, Shreveport, LA and Dr. P. Traber, University of Pennsylvania, Philadelphia, PA). The duodenum (first 5 cm distal to pyloroduodenal junction) was removed from adult animals and flushed gently with PBS. Tissue was frozen in O.C.T. embedding medium (Miles, Inc., Elkhart, IN) in hexane chilled on liquid nitrogen, and 7-μm sections were collected on poly-L-lysine-coated slides. After a brief thaw, slides were fixed for 2 minutes in 4% paraformaldehyde/PBS (0.1 mM $CaCl_2$) then washed twice with PBS (0.1 mM $CaCl_2$ in first wash). Tissues were permeabilized with TritonX-100 (0.1% in PBS), rinsed in PBS, and blocked with powdered milk (1% in PBS). Each of these steps was carried out at room temperature for 5 minutes. Sections were then incubated with primary antibody overnight at 37°C, washed in blocking solution (three times, 10 minutes each), and incubated with FITC-conjugated secondary antibody for 45 minutes at 37°C. Secondary antibodies used included goat anti-mouse IgG flourescein (Chemicon), goat anti-rabbit IgG (whole molecule) FITC conjugate (F-0511; Sigma, St. Louis, MO), and goat anti-rat IgG (whole molecule) FITC conjugate (F-6258; Sigma). All antibodies were diluted in powdered milk (1% in PBS). Final washes included 1% powdered milk-PBS (three times, 10 minutes each) and PBS (two times, 5 minutes each). Slides were mounted with Vectashield (Vector Laboratories, Burlingame, CA) and examined on a laser scanning-confocal microscope (Ultima, Meridian Instruments, Inc., Okemos, MI).

β-Galactosidase Expression

For wholemount staining of embryonic tissues, pregnant females from matings between heterozygous animals were killed by cervical dislocation at 13.5 dpc. Following removal of the fetuses from the uterus, heads were taken for DNA isolation and genotype confirmation by PCR. Fixation and X-gal (5-bromo-4-chloro-3-indolyl-β-D-galactoside) staining were performed as described previously (Bonnerot and Nicolas, 1993). Following staining, fetuses were postfixed in glutaraldehyde (1% in PBS) for 30 minutes at room temperature. Viscera were removed and photographed.

For staining of adult chimeric intestine, the proximal duodenum was removed from a male exhibiting 50% chimerism. The tissue was cut into 0.5-cm pieces, rinsed briefly in PBS, and frozen in O.C.T. on dry ice. Cryostat sections (7 μm) were placed directly into 0.5% glutaraldehyde fixative (containing 1.25 mM EGTA and 2 mM $MgCl_2$ in PBS) for 5 minutes. Slides were washed three times in wash buffer (2 mM $MgCl_2$ and 0.02% NP-40 in 0.1 M phosphate buffer, pH 7.3) for 5 minutes each and incubated in X-gal staining solution (1 mg/ml X-gal in N, N-dimethylformamide, 5 mM $K_3Fe(CN)_6$, 5 mM $K_4Fe(CN)_6$-$3H_2O$, and 2 mM $MgCl_2$) in wash buffer overnight at 37°C. Following three washes in wash buffer, slides were coverslipped and examined on a Leitz Orthoplan photomicroscope (Leitz, Inc., Rockleigh, NJ).

ACKNOWLEDGMENTS

We are grateful to Dr. Thom Saunders of the University of Michigan Transgenic Mouse Core for microinjection and transplantation of blastocysts. We also thank Dr. Michael Welsh and Mr. Chris Edwards for assistance with confocal microscopy; Ms. Karen Beningo and Drs. Joyce Vanderkuur and George Campbell for assistance with Western analyses; and Mr. Bruce Donohoe, Ms. Kaye Brabec, and Mr. Robert Crawford of the University of Michigan Morphology Core for assistance with electron microscopy and immunocytochemistry. Finally, we are grateful to Drs. K. Sue O'Shea and Sally Camper for technical advice, valuable discussion, and review of this paper. The University of Michigan Transgenic Animal Core is supported by the Centers for Organogenesis, Cancer (5P30CA46592), and Arthritis (5P60AR20557). D.L.G. is grateful for grant support from NIH R29 HD28620.

REFERENCES

Arpin M, Pringault E, Finidori J, Garcia A, Jeltsch J-M, Vandekerckhove J, Louvard D. Sequence of human villin: A large duplicated domain homologous with other actin-severing proteins and a unique small carboxy-terminal domain related to villin specificity. J. Cell Biol. 1988;107:1759–1766.

Arpin M, Friederich E, Algrain M, Vernel F, Louvard D. Functional differences between L- and T-plastin isoforms. J. Cell Biol. 1994;127: 1995–2008.

Berryman M, Gary R, Bretscher A. Ezrin oligomers are major cytoskeletal components of placental microvilli: A proposal for their involvement in cortical morphogenesis. J. Cell Biol. 1995;131:1231–1242.

Bonnerot C, Nicolas J-F. Applications of LacZ gene fusions to postimplantation development. Methods Enzymol. 1993;225:451–469.

Bradley A. Production and analysis of chimeric mice. In Robertson EJ, ed. Teratocarcinomas and Embryonic Stem Cells: A Practical Approach. Oxford: Oxford University Press, 1987:113–152.

Bretscher A. Fimbrin is a cytoskeletal protein that crosslinks F-actin in vitro. Proc. Natl. Acad. Sci. USA 1981a;78:6849–6853.

Bretscher A. Characterization and ultrastructural role of the major components of the intestinal microvillus cytoskeleton. Cold Spring Harbor Symp. Quant. Biol. 1981b;46:871–879.

Bretscher A, Weber K. Purification of microvilli and an analysis of the protein components of the microfilament core bundle. Exp. Cell Res. 1978;116:397–407.

Bretscher A, Weber K. Villin is a major protein of the microvillus cytoskeleton which binds both G and F actin in a calcium-dependent manner. Cell 1980;20:839–847.

Chafel MM, Shen W, Matsudaira P. Sequential expression and differential localization of I-, L-, and T-fimbrin during differentiation of the mouse intestine and yolk sac. Dev. Dyn. 1995;203:141–151.

Chambers C, Grey RD. Development of the structural components of the brush border in absorptive cells of the chick intestine. Cell Tissue Res. 1979;204:387–405.

Coluccio LM, Bretscher A. Reassociation of microvillar core proteins: Making a microvillar core in vitro. J. Cell Biol. 1989;108:495–502.

Costa de Beauregard, M-A, Pringault E, Robine S, Louvard D. Suppression of villin expression by antisense RNA impairs brush border assembly in polarized epithelial intestinal cells. EMBO J. 1995;14:409–421.

Craig SW, Lancashire CL. Comparison of intestinal brush-border 95-κdalton polypeptide and alpha-actinins. J. Cell Biol. 1980;84:655–667.

Craig SW, Powell LD. Regulation of actin polymerization by villin, a 95,000 dalton cytoskeletal component of intestinal brush borders. Cell 1980;22:739–746.

Doetschman T. Gene transfer in embryonic stem cells. In Pickert C, ed. Transgenic Animal Technology. A Laboratory Handbook. San Diego. Academic Press, 1994:115–146.

Dudouet B, Robine S, Huet C, Sahuquillo-Merino C, Blair L, Coudrier E, Louvard D. Changes in villin synthesis and subcellular distribution during intestinal differentiation of HT29-18 clones. J. Cell Biol. 1987;105:359–369.

Ezzell RM, Chafel MM, Matsudaira PT. Differential localization of villin and fimbrin during development of the mouse visceral endoderm and intestinal epithelium. Development (Cambridge) 1989;106: 407–419.

Ezzell RM, Leung J, Collins K, Chafel MM, Cardozo TJ, Matsudaira PT. Expression and localization of villin, fimbrin and myosin I in differentiating mouse F9 teratocarcinoma cells. Dev. Biol. 1992;151: 575–585.

Friederich E, Huet C, Arpin M, Louvard D. Villin induces microvilli growth and actin redistribution in transfected fibroblasts. Cell 1989;59:461–475.

Glenney JR, Weber K. Calcium control of microfilaments: Uncoupling of the F-actin severing and bundling activity of villin by limited proteolysis in vitro. Proc. Natl. Acad. Sci. USA 1981;78:2810–2814.

Glenney JR Jr, Kaulfus P, Matsudaira P, Weber K. F-actin binding and bundling properties of fimbrin, a major cytoskeletal protein of microvillus core filaments. J. Biol. Chem. 1981a;256:9283–9288.

Glenney JR Jr, Kaulfus P, Weber K. F-actin assembly modulated by villin: Ca^{++}-dependent nucleation and capping of the barbed end. Cell 1981b;24:471–480.

Gustin MC, Goodman DBP. Isolation of brush-border membrane from the rabbit descending colon epithelium. J. Biol. Chem. 1981;256: 10651–10656.

Heath JP. Epithelial cell migration in the intestine. Biol. Int. 1996;20: 139–146.

Heintzelman MB, Mooseker MS. Assembly of the intestinal brush border cytoskeleton. Curr. Topics Dev. Biol. 1992;26:93–122.

Janmey PA, Matsudaira PT. Functional comparison of villin and gelsolin. J. Biol. Chem. 1988;32:16738–16743.

Keller G, Kennedy M, Papayannopoulou T, Wiles MV. Hematopoietic commitment during embryonic stem cell differentiation in culture. Mol. Cell. Biol. 1993;13:473–486.

Kendall SK, Samuelson LC, Saunders TL, Wood RI, Camper SA. Targeted disruption of the pituitary glycoprotein hormone α-subunit produces hypogonadal and hypothyroid mice. Genes Dev. 1995;9: 2007–2019.

Kozak M. Interpreting cDNA sequences: Some insights from studies on translation. Mamm. Genome 1996;7:563–574.

Lin C-S, Park T, Chen ZP, Leavitt J. Human plastin genes. J. Biol. Chem. 1993;268:2781–2792.

Lin C-S, Shen W, Chen ZP, Tu Y-H, Matsudaira P. Identification of I-plastin, a human fimbrin isoform expressed in intestine and kidney. Mol. Cell. Biol. 1994;14:2457–2467.

Matsudaira P, Mandelkow E, Renner W, Hesterberg LK, Weber K. Role of fimbrin and villin in determining the interfilament distances of actin bundles. Nature (London). 1983;301:209–214.

Maunoury R, Robine S, Pringault E, Huet C, Guenet JL, Gaillard JA, Louvard D. Villin expression in the visceral endoderm and the gut anlage during early mouse embryogenesis. EMBO J. 1988;7:3321–3329.

Maunoury R, Robine S, Pringault E, Leonard N, Gaillard JA, Louvard D. Developmental regulation of villin gene expression in the epithelial cell lineages of mouse digestive and urogenital tracts. Development (Cambridge). 1992;115:717–728.

Maupin-Szamier P, Pollard TD. Actin filament destruction by osmium tetroxide. J. Cell Biol. 1978;77:837–852.

Mooseker MS. Organization, chemistry, and assembly of the cytoskeletal apparatus of the intestinal brush border. Annu. Rev. Cell Biol. 1985;1:209–241.

Nagy A, Rossant J, Nagy R, Abramow-Newerly W, Roder JC. Derivation of completely cell culture-derived mice from early-passage embryonic stem cells. Proc. Natl. Acad. Sci. USA 1993;90:8424–8428.

O'Kane S, Witke W, Kwiatkowski DJ, Deakin A, Ferguson MWJ. Wound healing in the gelsolin knockout mouse: evidence that

cytoskeletal factors are important in scar formation. Mol. Biol. Cell. 1996;7:543a

Pringault E, Robine S, Louvard D. Structure of the human villin gene. Proc. Natl. Acad. Sci. USA 1991;88:10811–10815.

Ramirez-Solis R, Rivera-Perez J, Wallace JD, Wims M, Zheng H, Bradley A. Genomic DNA microextraction: A method to screen numerous samples. Anal. Biochem. 1992;201:331–335.

Rousseau-Merck MF, Simon-Chazottes D, Arpin M, Pringault E, Louvard D, Guenet JL, Berger R. Localization of the villin gene on human chromosome 2q35-q36 and on mouse chromosome 1. Hum. Genet. 1988;78:130–133.

Schmidt GH, Winton DJ, Ponder BJ. Development of the pattern of cell renewal in the crypt-villus unit of chimaeric mouse small intestine. Development (Cambridge). 1988;103:785–790.

Small JV, Langanger G. Organization of actin in the leading edge of cultured cells: Influence of osmium tetroxide and dehydration on the ultrastructure of actin meshworks. J. Cell Biol. 1981;91:695–705.

Witke W, Sharpe AH, Hartwig JH, Azuma T, Stossel TP, Kwiatkowski DJ. Hemostatic, inflammatory, and fibroblast responses are blunted in mice lacking gelsolin. Cell 1995;81:41–51.

Wurst W, Joyner AL. Production of targeted embryonic stem cell clones. In Joyner AL, ed. Gene Targeting: A Practical Approach. Oxford. IRL Press, 1993:36–38.